

J0316+4328: a Probable “Asymmetric Double” Lens

E. R. Boyce^{1*}, S. T. Myers², I. W. A. Browne¹, W. J. Stroman^{2,3} and N. J. Jackson¹

¹*University of Manchester, Jodrell Bank Observatory, Macclesfield, Cheshire SK11 9DL*

²*National Radio Astronomy Observatory, PO Box O, Socorro, NM 87801, United States*

³*Iowa State University, Department of Physics and Astronomy, 12 Physics Hall, Ames, IA 50011, United States*

Accepted 2007 July 16. Received 2007 June 30; in original form 2007 June 04

ABSTRACT

We report a probable gravitational lens J0316+4328, one of 19 candidate asymmetric double lenses (2 images at a high flux density ratio) from CLASS. Observations with the Very Large Array (VLA), MERLIN and the Very Long Baseline Array (VLBA) imply that J0316+4328 is a lens with high confidence. It has 2 images separated by 0''.40, with 6 GHz flux densities of 62 mJy and 3.2 mJy. The flux density ratio of ~ 19 (constant over the frequency range 6–22 GHz) is the largest for any 2 image gravitational lens. High resolution optical imaging and deeper VLBI maps should confirm the lensing interpretation and provide inputs to detailed lens models. The unique configuration will give strong constraints on the lens galaxy’s mass profile.

Key words: gravitational lensing – cosmology:miscellaneous.

1 INTRODUCTION

Galaxy-scale gravitational lenses are valuable tools for the study of galactic structure. The locations and brightnesses of the images provide constraints on the overall lens galaxy profile, while remaining anomalies and time variations in the brightnesses due to micro-lensing probe substructure on scales from dark matter clumps (Mao & Schneider 1998; Dalal & Kochanek 2002) and satellite galaxies (McKean et al. 2007) to stars (Schechter & Wambsgans 2002). Lens images are sensitive to the surface densities at the locations where they form, generally at galactocentric radii of a few kpc for bright lens images. Measuring the overall lens galaxy profile over a range of scales requires more information, which can be provided by stellar velocity dispersions at radii < 1 kpc (Koopmans et al. 2006) or weak lensing at radii of tens of kpc (Gavazzi et al. 2007). Lenses with central images measure the density profile on many scales using strong lensing alone, giving strong constraints at radii of ~ 100 pc, including any contribution from a central super-massive black hole (Winn et al. 2004).

For lensed quasars, the best measurement of the lens galaxy profile can be done if the quasar is radio-loud. The size of the emitting region is larger in the radio than in optical or X-ray (Koopmans & de Bruyn 2000), making the image brightnesses less susceptible to microlensing, while central images are strongly affected by dust absorption and confusion in the optical regime but not in the radio frequency range 5–40 GHz (Winn et al. 2004). The largest sample of radio-loud lenses has been provided by CLASS (Myers et al.

2003; Browne et al. 2003), which found 22 instances of a bright radio source lensed by a foreground galaxy.

A crucial step in CLASS was the rejection of double sources with a flux density ratio $> 10 : 1$ (Myers et al. 2003) after the initial 8.4 GHz VLA snapshot. This was done for two reasons; for statistical completeness of the lens sample it was necessary to be sure that all secondary components could be detected reliably and it also significantly reduced the amount of follow-up observations required. A secondary compact component of similar brightness to the primary is likely to be a lensed image, while a secondary component much fainter than the primary is most likely to be weak structure belonging to the primary source. This strategy necessarily excluded “asymmetric doubles”: 2 image lenses with a high flux density ratio. Such lenses are of interest because they are most likely to host observable central images (Mao et al. 2001; Bowman et al. 2004), while even the absence of a central image gives the strongest constraints in an asymmetric double (Rusin & Ma 2001; Boyce et al. 2006; Zhang et al. 2007). Though the recognition of weak secondaries with ratios $> 10 : 1$ in CLASS may not have been 100% reliable, many are detectable. We have, therefore, conducted a program to identify such lenses by following up promising candidates which were initially rejected only on the basis of a high flux density ratio.

2 SURVEY AND OBSERVATIONS

We selected 18 candidates which were fitted by multiple compact components in the initial CLASS VLA snapshots, and for which the second brightest component was 10 – 30

* E-mail: edward.boyce@manchester.ac.uk (ERB)

Table 1. Summary of VLA observations. Flatter and steeper refer to the spectral indices of weaker components over the observed frequencies, relative to the primary compact source. e.g. J0008+6837 had 2 compact radio components, the fainter of these had a steeper radio spectrum between 5 and 8.5 GHz. Most of our candidates were typical radio sources with a flat-spectrum, compact core and a steeper spectrum, often extended, lobe or knot in a jet. Only J0316+3350, J0935+0719 and J0958+2948 could be considered lens candidates from the VLA observations.

Source	R.A. (J2000)	Dec.	Observing Time (mins.)			Notes
			5 GHz	8.5 GHz	22 GHz	
J0008+6837	00 08 33.5	68 37 22	14	14	-	Rejected: 2nd component steeper
J0152+3350	01 52 34.6	33 50 33	6	8	-	Rejected: 2nd component steeper
J0316+3350	03 16 50.9	43 28 19	11	12	17	Possible Lens from VLA observations
J0644+5955	06 44 04.7	59 55 21	6	7	-	Rejected: 2nd and 3rd components extended, steeper
J0812+4041	08 12 03.0	40 41 08	18	18	-	Rejected: 2nd and 3rd components extended, steeper
J0852+5922	08 52 30.0	59 22 50	18	19	-	Rejected: 2nd component extended, steeper
J0903+4651	09 03 04.0	46 51 04	4	5	45	Rejected: 2nd component extended
J0935+0719	09 35 01.1	07 19 19	12	14	23	Possible Lens from VLA observations
J0938+3934	09 38 39.2	39 34 20	18	18	-	Rejected: 2nd component extended, steeper
J0958+2948	09 58 58.9	29 48 04	12	13	21	Possible Lens from VLA observations
J1131+5146	11 31 16.5	51 46 34	18	19	-	Rejected: 2nd component extended, steeper
J1252+1910	12 52 27.8	19 10 38	18	19	-	Rejected: 2nd component extended, steeper
J1253+6304	12 53 17.5	63 04 36	18	18	24	Rejected: 2nd component flatter, 3rd component extended
J1343+2844	13 43 00.2	28 44 07	6	6	-	Rejected: 2nd component extended, steeper
J1540+1447	15 40 49.5	14 47 46	4	5	28	Rejected: 2nd component extended, steeper
J1641+5115	16 41 55.7	51 15 47	9	10	-	Rejected: 2nd component extended, steeper
J2139+1027	21 39 42.6	10 27 43	7	7	14	Rejected: 2nd component steeper
J2353+3231	23 53 20.9	32 31 44	14	14	-	Rejected: 2nd component extended, steeper

times fainter than the brightest. New observations of these sources were made with the VLA in A configuration at 5 and 8.5 GHz on 2006 February 12 and 2006 February 19. Each source was observed for a few minutes in several blocks at different hour angles, giving better u-v coverage than the initial snapshots. Candidates with multiple compact components at 5 and 8.5 GHz were re-observed at 22 GHz on 2006 March 20 or 2006 April 03. Most candidates were found to have an extended secondary component, or differing spectral indices between components, leaving 3 candidates as possible lenses, J0316+4328, J0935+0719 and J0958+2948. The observations are summarised in Table 1.

J0958+2958 has 2 compact radio sources separated by $8''$, but these objects are distinct quasars with redshifts of 2.064 and 2.744, ruling out this system as a gravitational lens (Lehár et al. 2001). J0935+0719 has a series of radio observations indicating that it might be a gravitational lens in which the source is a compact symmetric object, and is mentioned as the candidate J0935+073 in Browne et al. (2003). We find that the flux density ratio is 19:1 at 5, 8.5 and 22 GHz, supporting the lensing interpretation. A definitive answer on the nature of J0935+0719 requires better optical data, both imaging and spectroscopic, and we do not consider this system further in this paper.

This left J0316+4328 as a possible candidate lacking high resolution radio imaging. After completing the longer VLA observations we realised that another source, J0856+4935, looked promising in the initial CLASS snapshot. On December 08 2006 and December 09 2006 we observed both sources at 6.0 GHz with the Multiple Element Radio-Linked Interferometric Network (MERLIN), spending 12 hours on each source. J0856+4935 had a diffuse secondary component and was rejected as a lens, while J0316+4328 showed 2 compact components and remained as a lens candidate with increased confidence.

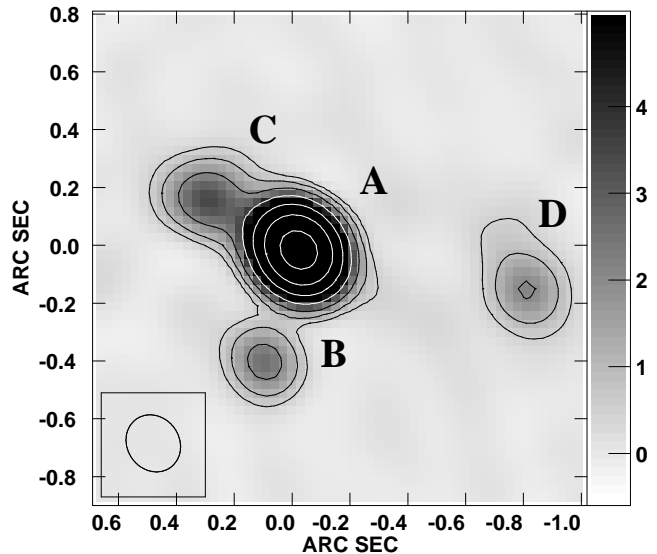


Figure 1. 8.5 GHz VLA A array map of J0316+4328, made with super-uniform weighting. Components A and B are probably 2 images of a lensed quasar, with a flux density ratio of 17.0 ± 0.6 . C and D are probably lobes situated either side of the quasar core which lie too far from the lensing galaxy to form multiple images. The off-source rms is 0.09 mJy/beam and the beam is $0''.20 \times 0''.18$ at a position angle of 35° . The co-ordinates are offset from 03 16 50.933 +43 28 19.31, the greyscale is in mJy/beam, and the contours increase in factors of 2 from 0.5 mJy/beam.

The maps of J0316+4328 with the VLA and MERLIN are presented as Figures 1, 2 and 3, while fits to the components are presented in Table 2. We also mapped the system in Stokes Q, U and V, using the MERLIN data, and detected no polarised emission at an rms of 0.13 mJy/beam.

Table 2. Gaussian fits to the components of J0316+4328, giving positions relative to component A in the 22 GHz VLA map, integrated flux densities and sizes (deconvolved major axes). Components C and D were clearly resolved in the 6.0 GHz MERLIN map (see Figure 3), so in this case 2 gaussians were fitted. The flux density is the total flux density of the 2 components, the size is their separation. B is unresolved in each map, while A is marginally resolved with MERLIN. The off-source rms values were 0.13, 0.09 and 0.09 mJy/beam and the beam sizes were $0''.051 \times 0''.045$, $0''.20 \times 0''.18$ and $0''.11 \times 0''.07$ in the 6.0, 8.5 and 22.5 GHz maps, respectively.

Component	R.A.	Dec.	6.0 GHz MERLIN		8.5 GHz VLA		22.5 GHz VLA	
			Size	S (mJy)	Size	S (mJy)	Size	S (mJy)
A	$0''.00$	$0''.00$	$0''.051$	61.91	$0''.06$	45.75	$0''.05$	26.60
B	$0''.11$	$-0''.38$	$0''.017$	3.23	$0''.05$	2.69	$0''.05$	1.36
C	$0''.32$	$0''.18$	$0''.09$	5.26	$0''.17$	4.89	$0''.15$	2.09
D	$-0''.76$	$-0''.12$	$0''.07$	4.08	$0''.21$	3.25	$0''.29$	1.21

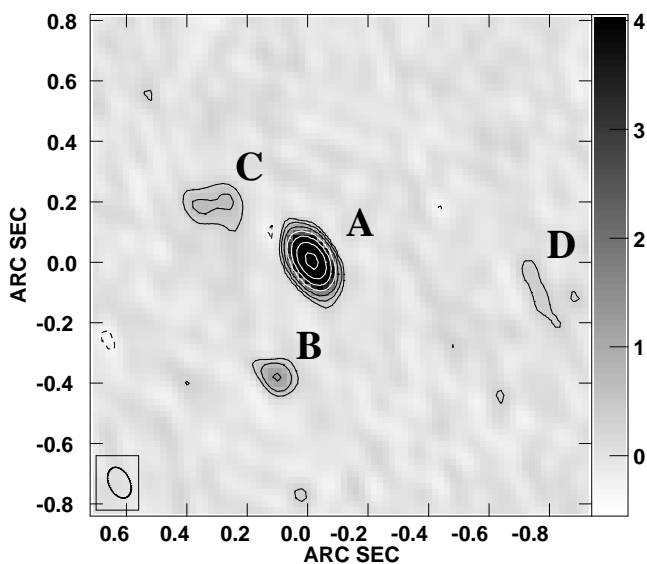


Figure 2. 22.5 GHz VLA A array map of J0316+4328. Components A and image B are both compact, with a flux density ratio of 19.6 ± 1.3 . With higher resolution, components C and D are clearly extended. The off-source rms is 0.09 mJy/beam and the beam is $0''.11 \times 0''.07$ at a position angle of 25° . The coordinates are offset from 03 16 50.933 +43 28 19.31, the greyscale is in mJy/beam, and the contours increase in factors of 2 from 0.3 mJy/beam.

J0316+4328 has 2 compact components (A and B) with flux density ratios of 19.6 ± 1.3 , 17.0 ± 0.6 , 19.2 ± 0.8 at 6.0 GHz, 8.5 GHz and 22 GHz, respectively. Errors are $1-\sigma$ values taken from the map rms. The 2 steeper spectrum components (C and D) either side of A and B are extended with the VLA and clearly resolved by MERLIN. These are probably lobes situated either side of the radio source's core which lie too far from the lensing galaxy to be multiply imaged.

We observed J0316+4328 with the Very Long Baseline Array (VLBA) at 8.4 GHz on 2006 July 16. The observation was made at an observing rate of 256 Mb/s and included 113 minutes on J0316+4328. Self-calibration was used to derive the phase solutions, and it was not possible to fit good solutions on the longest baselines, so the Mauna Kea, St. Croix and Hancock antennas were omitted. Components A and B (Figures 4 and 5) were found to have reduced flux densities compared to those in the VLA maps (Table 3), presumably due to resolving out extended emission. No emission was de-

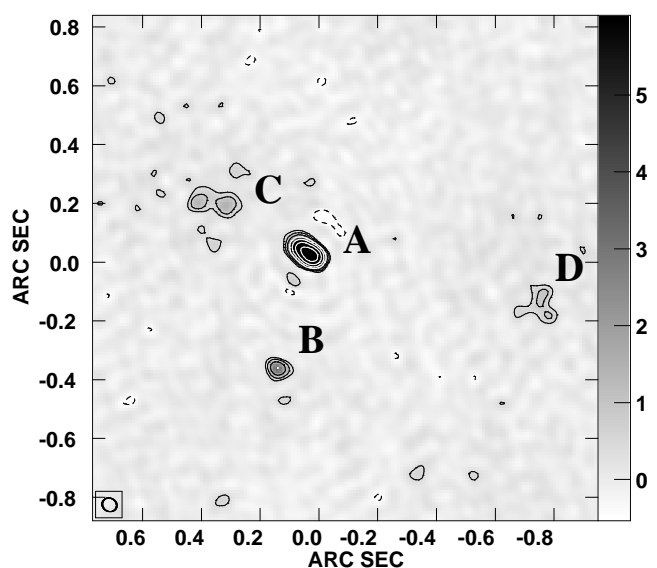


Figure 3. 6.0 GHz MERLIN map of J0316+4328. Component B is compact, component A is marginally extended (major axis $0''.051$ at a position angle of 54°). The flux density ratio of components A and B is 19.2 ± 0.8 , taking the total flux density of A. Components C and D are resolved by MERLIN. The off-source rms is 0.13 mJy/beam and the beam is $0''.051 \times 0''.045$ at a position angle of 61° . The co-ordinates are offset from 03 16 50.93 +43 28 19.3, the greyscale is in mJy/beam, and the contours increase in factors of 2 from 0.4 mJy/beam.

tected at the locations of components C and D; they were completely resolved out by the VLBA. Component A has 84% of its flux density in a central point source A1 and the remainder in jet components A2 and A3. Component B has a single point source sub-component B1, with a flux density ratio relative to A1 of 23.7 ± 1.5 , matching the 6 GHz and 22 GHz ratios at the $2-\sigma$ level.

Some simple lens models which fit the bright images place the central image only ~ 20 mas from image B. While these models are severely underconstrained (due to the dearth of information on the lens galaxy), it is plausible that the VLA and MERLIN maps would blend image B with the central image, meaning that only the VLBA maps constrain the central image. No source was seen between images A and B, with a $5-\sigma$ limit of 0.33 mJy, although interpreting a non-detection over many resolution elements is not straightforward, see Zhang et al. (2007).

Table 3. Gaussian fits to the components of J0316+4328 in the VLBA maps, giving positions relative to A1, integrated flux densities and sizes (deconvolved major axes). The blank field rms values were (0.08,0.065) mJy/beam in the A and B fields, respectively. The beam size was 2.8×2.5 mas. A1, A2 and B1 are compact.

	R.A. (mas)	Dec. (mas)	Size (mas)	S (mJy)
A1	0.0	0.0	1.3	23.7
A2	5.4	4.9	2.2	1.6
A3	34.1	25.9	4.5	3.0
B1	120.4	-379.9	0.0	1.0

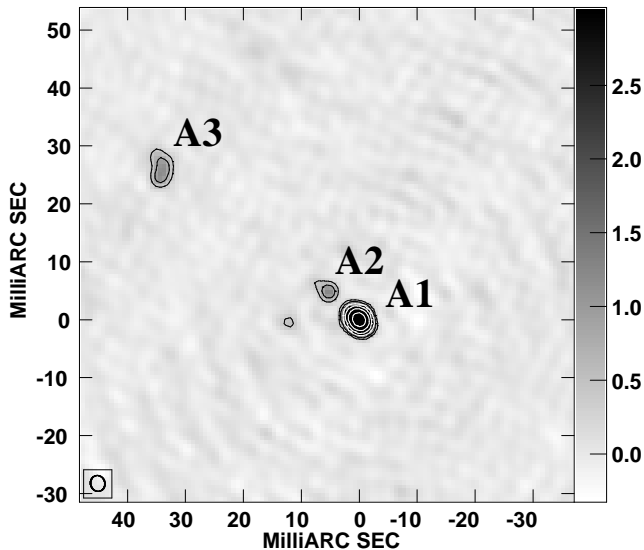


Figure 4. 8.4 GHz VLBA map of the A component in J0316+4328, omitting the Mauna Kea, Hancock and St. Croix antennas. At VLBI scales component A splits into an unresolved core A1 and jet components A2 and A3 at distances of 7 and 43 mas and position angles of 48° and 53° , respectively. This matches the 51 mas size and 54° position angle of component A in the 6.0 GHz MERLIN map (Figure 3). The off-source rms is 0.08 mJy/beam and the beam is 2.8×2.5 mas at a position angle of 16° . The co-ordinates are offset from component A1, the greyscale is in mJy/beam, and the contours increase in factors of 2 from 0.4 mJy/beam.

3 DISCUSSION

Although we lack high-resolution optical data, we are very confident that J0316+4328 is a gravitational lens. Components A and B are very likely to be lensed images of the same quasar, as they are compact at resolutions from $0''.2$ to $0''.05$ and exhibit the same flux density ratio over a factor of 3.5 in frequency (Figure 6). At 3 mas resolution substructure is seen only in the brighter, more magnified image. All but one of the CLASS candidates with multiple compact components in VLBA maps were confirmed as lenses (Browne et al. 2003). The exception, B0827+525, had significantly different spectra for the 2 components and is likely to be a binary quasar (Koopmans et al. 2000).

We plan to obtain a VLBI map with rms ~ 0.02 mJy, which would definitively confirm the lensing interpretation by detecting parity-reversed substructure in image B matching that in image A. If B is a lensed image 19 times fainter than A, it should include sub-components B2 and B3 with

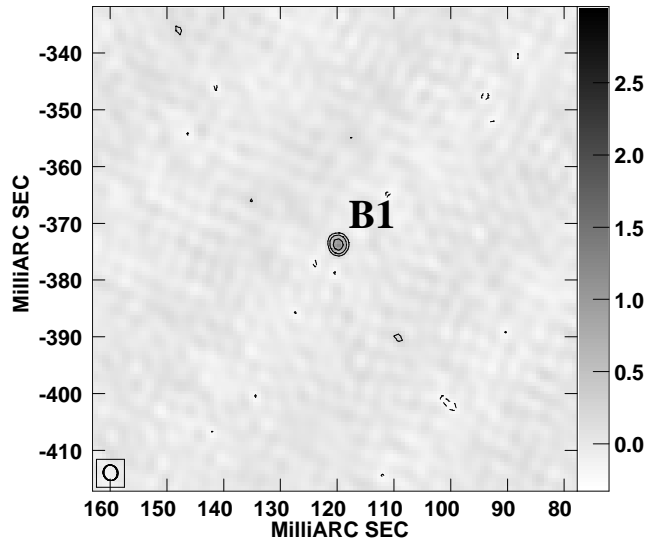


Figure 5. 8.4 GHz VLBA map of the B component in J0316+4328, omitting the Mauna Kea, Hancock and St. Croix antennas. It appears as a single compact point source B1, with a flux density ratio relative to A1 of 23.7 ± 1.5 . The off-source rms is 0.065 mJy/beam and the beam is 2.8×2.5 mas at a position angle of 16° . The co-ordinates are offset from the brightest component A1 (shown in Figure 4), the greyscale is in mJy/beam, and the contours increase in factors of 2 from 0.2 mJy/beam.

flux densities of 0.08 and 0.16 mJy, and separations from B1 of 1.7 and 10 mas. This map would also improve the flux density measurement of B1 (which currently limits the precision of the VLBI flux density ratio), and might even detect a central image.

We are also pursuing high resolution optical images with the William Herschel telescope and spectroscopic observations with the Lick telescope. The USNO B1 catalog shows an optical object with $R=19.1$ and $B=20.3$ at 03 16 50.8693 +43 28 19.880, an offset of $-0''.69$ in right ascension and $+0''.55$ in declination from image A in the MERLIN map. The USNO catalog has astrometric accuracy of $0''.20$ (Monet et al. 2003) and this object has errors of $0''.38$ in right ascension and $0''.10$ in declination, while the MERLIN map has astrometric accuracy and positional error both better than $0''.05$. The optical and radio positions are consistent at the $2\text{-}\sigma$ level, but it is not possible to identify the USNO object as a lensed image, the lens galaxy, or a blend of both. High resolution optical images should confirm the lensing interpretation, and allow detailed lens modelling.

For isothermal profiles with moderate ellipticity or

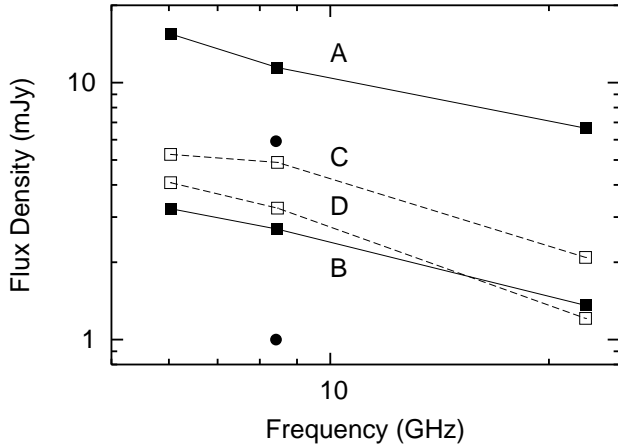


Figure 6. Spectra of the components of J0316+4328 from the VLA and MERLIN observations. A and B (solid squares, solid lines) have the same spectrum from 6 GHz to 22 GHz, while C and D (hollow squares, dashed lines) are noticeably steeper. The VLBA flux densities of A1 and B1 are plotted as solid circles. Component A and A1 flux densities are multiplied by 0.25.

shear, the lensing cross-section for asymmetric doubles (magnification ratio 10 – 20) is $\sim 20\%$ that of quads and symmetric doubles (magnification ratio 1 – 10) combined. With 21 quad or symmetric double lenses in CLASS, 4-5 asymmetric doubles would be expected. 3 such systems have been found, counting the confirmed lens B1030+074 and the 2 strong candidates J0316+4328 and J0935+0719.

Our lens modelling must accommodate the extended, steep-spectrum components C and D. Their radio spectra are different from each other as well as from A and B (Figure 6), and their separation is $1''.12$ as opposed to $0''.40$ for images A and B, so C and D are unlikely to be a pair of lens images. Their orientation either side of image A, and the fact that substructure in A points towards the brighter component C, argues that they are diffuse lobes lying either side of the source’s core, in a typical double radio source configuration. With the lens image separation of $0''.40$ arguing for a relatively less massive lens galaxy with a small lensing cross-section, it should be possible to find models where the source’s lobes lie outside the multiply-imaged region of the source plane, while the core lies just within it. The configuration actually resembles that of the first lens system B0957+561 (Walsh, Carswell, & Weymann 1979; Roberts, Greenfield, & Burke 1979).

Our modelling will give strong constraints on the lens galaxy’s density profile. For near isothermal models which are a good approximation to most lens galaxies (Rusin et al. 2003; Koopmans et al. 2006), images A and B form at radii differing by a factor of 15-20 and constrain the density profile over this large range of galactocentric radius. The constraints will be particularly strong if substructure is detected in each image, as in the case of B1152+199 (Rusin et al. 2002). Also, central images become brighter as image B becomes fainter, relative to image A. Compared to quad or symmetric double lenses, J0316+4328 is more likely to show a central image in sensitive VLBI maps, and even an upper limit on the central image flux density will be a more stringent model constraint.

4 CONCLUSION

We have detected a probable gravitational lens with 2 bright images at a considerably higher flux density ratio than any previously known double lens. Improved VLBI and high-resolution optical observations are underway. This highly asymmetric lens should give unusually stringent constraints on the density profile of the lens galaxy.

5 ACKNOWLEDGMENTS

MERLIN is a National Facility of STFC operated by the University of Manchester. The National Radio Astronomy Observatory is a facility of the National Science Foundation operated under cooperative agreement by Associated Universities, Inc. Support for WJS and the VLBA observation of J0316+4328 were provided by the Research Experience for Undergraduates program at NRAO. This work was supported in part by the European Community’s Sixth Framework Marie Curie Research Training Network Programme, Contract No. MRTN-CT-2004-505183 ”ANGLES.”

REFERENCES

- Bowman, J. D., Hewitt, J. N., Kiger, J. R., 2004, *ApJ*, 617, 81
- Boyce, E. R., Winn, J. N., Hewitt, J. N., Myers, S. T., 2006, *ApJ*, 648, 73
- Browne, I. W. A., et al., 2003, *MNRAS*, 341, 13
- Dalal, N., Kochanek, C. S., 2002, *ApJ*, 572, 25
- Gavazzi R., Treu T., Rhodes J. D., Koopmans L. V. E., Bolton A. S., Burles S., Massey R., Moustakas L. A., 2007, *ApJ*, accepted, arxiv.org:astro-ph/0701589
- Koopmans, L. V. E., de Bruyn, A. G., 2000, *A&A*, 358, 793
- Koopmans L. V. E., et al., 2000, *A&A*, 361, 815
- Koopmans, L. V. E., Treu, T., Bolton, A. S., Burles, S., Moustakas, L. A., 2006, *ApJ*, 649, 599
- Lehár, J., Buchalter, A., McMahon, R. G., Kochanek, C. S., Muxlow, T. W. B., 2001, *ApJ*, 547, 60
- Mao, S., Schneider, P., 1998, *MNRAS*, 295, 587
- Mao, S., Witt, H. J., Koopmans, L. V. E., 2001, *MNRAS*, 323, 301
- McKean, J. P., et al., 2007, *MNRAS*, 378, 109
- Monet D. G., et al., 2003, *AJ*, 125, 984
- Myers, S. T., et al., 2003, *MNRAS*, 341, 1
- Roberts D. H., Greenfield P. E., Burke B. F., 1979, *Sci*, 205, 894
- Rusin, D., Ma, C.-P., 2001, *ApJ*, 549, L33
- Rusin D., Norbury M., Biggs A. D., Marlow D. R., Jackson N. J., Browne I. W. A., Wilkinson P. N., Myers S. T., 2002, *MNRAS*, 330, 205
- Rusin, D., Kochanek, C. S., Keeton, C. R., 2003, *ApJ*, 595, 29
- Schechter, P. L., Wambsganss, J., 2002, *ApJ*, 580, 685
- Walsh D., Carswell R. F., Weymann R. J., 1979, *Natur*, 279, 381
- Winn, J. N., Rusin, D., Kochanek, C. S., 2004, *Natur*, 427, 613
- Zhang, M., Jackson, N., Porcas, R. W., Browne, I. W. A., 2007, *MNRAS*, accepted, arXiv:astro-ph/0703226